



Synthesis, Biological Activity, and the Effect of Ionization Radiation on the Spectral, XRD, and TGA Analysis of Cu(I), Cu(II), Zn(II), and Cd(II) Complexes

Samar A. Aly¹ · Safaa S. Hassan² · Hanaa A. El-Boraey³ · Ayman Eldourghamy¹ · Ehab M. Abdalla⁴ · Fahad M. Alminderej⁵ · Hussein H. Elganzory⁵

Received: 19 November 2022 / Accepted: 17 May 2023 / Published online: 7 August 2023

© The Author(s) 2023

Abstract

New complexes of molecular formulae of [Cu(H₂L₁)I] (B₁), [Cu(H₂L)₂(ClO₄)₂](B₂), [Zn (H₂L)₂(H₂O)]SO₄(B₃) and [Cd(H₂L)Cl]Cl(B₄) of ligand *N*-phenyl-2-(*p*-tolylglycyl)hydrazine -1-carbothioamide (B) have been prepared and characterized by ¹H-NMR, Mass spectra, FT-IR, elemental analyses, molar conductance, UV–visible spectra, magnetic susceptibility measurements, thermogravimetric analysis (TGA/DTG) and X-ray powder diffraction before and after irradiation. Elemental analyses indicate that the metal complexes have 1:1 (metal/ ligand) (B₁ and B₄) or 1:2 stoichiometry for complexes (B₂ and B₃). The results confirmed that gamma ray enhanced the stability of irradiated compounds as compared to non-irradiated compounds. XRD patterns proved that increasing the crystallinity of the samples and the particles is in nanosize range before and after gamma irradiation. These studies revealed that Cu(II) and Zn(II) complexes adopted octahedral geometry, and Cu(I) and Cd(II) complexes were found to be tetrahedral. The theoretical conformational structure analyses were performed using density functional theory for ligand and complexes at B3LYP functional with 6–31G basis set for ligand and LANL2DZ basis set for complexes. The ligand (B, A) and complexes (B₁–B₄) and (A₁–A₄) before and after irradiated have been tested for their inhibitory effect on the growth of bacteria against gram-positive (*Streptococcus pyogenes*) and gram-negative (*Escherichia coli*). Molecular docking investigation proved that the Zn(II) complex had interesting interactions with active site amino acids of topoisomerase II DNA gyrase enzymes (code: 2XCT).

Keywords Complexes · γ -irradiation · DFT calculations · Anti-bacteria · Molecular docking

✉ Samar A. Aly
samar.mostafa@gebri.usc.edu.eg

✉ Safaa S. Hassan
hsafaa@sci.cu.edu.eg

✉ Fahad M. Alminderej
f.alminderej@qu.edu.sa

✉ Hussein H. Elganzory
hhsien@qu.edu.sa

Hanaa A. El-Boraey
hanaaelborai@science.menofia.edu.eg

Ayman Eldourghamy
ayman.eldourghamy@gebri.usc.edu.eg

Ehab M. Abdalla
Ehababdalla99@sci.nvu.edu.eg

¹ Department of Environmental Biotechnology, Genetic Engineering and Biotechnology Research Institute, University of Sadat City, Sadat City 32958, Egypt

1 Introduction

Thiosemicarbazones are compounds which have increased importance over the decades as prospective medicine candidates. When coordinated to elements, they have evidenced as good antitumor, antimicrobial, antioxidant and antiprotozoal managers. Transition element created complexes that hold several advantages over other metal chelated because

² Chemistry Department, Faculty of Science, Cairo University, Giza 12613, Egypt

³ Chemistry Department, Faculty of Science, Menoufia University, Shebin El- Kom 32511, Egypt

⁴ Chemistry Department, Faculty of Science, New Valley University, Alkharga 72511, Egypt

⁵ Department of Chemistry, College of Science, Qassim University, Buraidah 51452, Saudi Arabia



of their good acceptability and decreased toxicity in living organisms [1, 2]. Thiosemicarbazone compound is of diverse importance for the reason that of their useful for living and pharmacological activities. Thiosemicarbazone derivatives have found application in drug development for the treatment of central nervous system disorders, of bacterial infection, as well as analgesic and antiallergic agent. Thiosemicarbazones are potent intermediates for the synthesis of pharmaceutical and bioactive materials, and thus, they are used extensively in the field of medicinal chemistry. Moreover, thiosemicarbazones have found their way into almost every branch of chemistry; commercially, they are used as dyes, photographic films, plastic and in textile industry [3]. The biological activity of these compounds depends upon the starting materials and their reaction conditions, also related to molecular conformation in particular, which can also be significantly affected by the presence of intra- and intermolecular hydrogen bonding [4]. Thiosemicarbazones commonly perform such as chelating compound for metal ions, attachment through (C=S) and (C=N-) groups, although in several cases they behave as monodentate compound where they bind through (C=S) only [5]. A series of copper(II) complexes of 2-phenylamino acetyl-*N*-phenyl hydrazine carbothioamide (H₂L) have been prepared and characterized by chemical and physical studies. The thermal behaviors of these chelates before and after γ -irradiation show that the complexes have induced more thermal stability after γ -irradiation. Solid state dc electrical conductivity for complexes was investigated before and after γ -irradiation [6, 7]. Recently, complexes of VO²⁺, Mn²⁺, Zn²⁺, Ru³⁺, Pd²⁺, Ag⁺ and Hg²⁺ have been prepared by reacting their metal salts with ligand (4-(4-chlorophenyl)-1-(2-(phenylamino) acetyl) thiosemicarbazone). Structure of synthesized metal complexes was confirmed by different analytical and spectral techniques (¹H NMR, MS, FT-IR, UV-Vis, EPR and Powder X-ray diffraction), thermogravimetric studies as well as molecular modeling. X-ray diffraction pattern of Mn²⁺, Pd²⁺ and Ag⁺ complexes before and after irradiation is recorded. The TGA studies of unirradiated and irradiated complexes showed that irradiated complexes were more thermally stable than unirradiated. The compound and its metal complexes have been examined for their inhibitory outcome on the growth of microorganisms against gram positive and gram negative [8–11]. In this work, we described the synthesis, characterization, DFT, molecular docking as well as antibacterial activities of Cu(I), Cu(II), Zn(II) and Cd(II) of complexes of ligand *N*-phenyl-2-(*p*-tolylglycyl)hydrazine-1-carbothioamide (B).

2 Materials and Methods

2.1 Materials

All chemicals used in this study were analytically reagent grade, commercially available from Fulka, and used without previous purification as CuI (anhydrous), Cu(ClO₄)₂, ZnSO₄, and CdCl₂ compounds which represent the metal ions (anhydrous), complexation process. All solvents were used as it is without previous purifications.

2.2 Synthesis of Thiosemicarbazide Ligand (B)

The organic ligand *N*-phenyl-2-(*p*-tolylglycyl)hydrazine-1-carbothioamide (B) was prepared by mixing equimolar amount of desired hydrazide (0.01 mol) in 10 ml of absolute ethanol and the appropriate amount of phenyl isothiocyanate in 10 ml of absolute EtOH [6]. The reaction mixture was reflux for 6 h. After cooling, the resulting precipitate was filtered off, washed several times with ethanol and diethyl ether and dried in vacuum in the presence of P₄O₁₀.

2.3 Synthesis of Metal Complexes

The metal complexes were prepared by adding to hot absolute ethanol solution (~ 20 mL) MX₂.*n*H₂O where M = Cu(I) and Cu(II), Zn(II), Cd(II), and X = I⁻, ClO₄⁻, SO₄⁻ and Cl⁻, *n* = 0–1 in appropriate molar ratio. The resulting mixture was magnetically stirred at 60 °C for 6–8 h. The formed precipitate was filtered off while hot; otherwise, the solution was left at 35 °C to evaporate some of solvent to promote crystallization. The crystals were collected by vacuum filtrations, washed several times with anhydrous diethyl ether and dried under vacuum in the presence of P₄O₁₀.

2.4 Physical Measurements

Elemental analyses (C, H and N) were performed at Microanalytical unit, Cairo University. Metal and halide analyses were estimated using standard literature methods [12]. The Fourier Transform Infrared (FT-IR) measurements were performed (4000–400 cm⁻¹) in KBr disks using Neneus-Nicolidite-640-MSA FT-IR, Thermo-Electronics Co. The UV-visible absorption spectra were measured in DMF solution using 4802 UV/vis double beam spectrophotometer. The ¹H-NMR spectra have been recorded in DMSO-d₆ as a solvent using Varian Gemini 200 NMR spectrophotometer and Varian-Oxford Mercury at 300 MHz, respectively. Mass spectra were acquired using the electron impact (EI) ionization technique at 70 eV on a Hewlett-Packard MS-5988 GC-MS instrument at the Microanalytical Center, National Research Centre, Egypt. Thermal analysis (TG/DTG) was

obtained out by using a Shimadzu DTA/TG-50 Thermal Analyzer with heating rate of 10 °C/min in nitrogen atmosphere with a following rate 20 mL/min in the range of ambient temperature up to 800 °C using platinum crucibles. X-ray powder diffraction analyses of solid samples were measured using APD 2000 PROModel GNR-X-ray Diffractometer at (NRC, Tanta University, Egypt). X-ray diffractograms give computer control formally finished by PHILIPS@MPDX'PERT X-ray diffractometer ready with Cu radiation $\text{CuK}\alpha$ ($\lambda = 1.54056 \text{ \AA}$). The X'pert diffractometer has the Bragg-Brentano geometry. The x-ray tube used was a copper tube operating at 40 kV and 30 mA. The scanning range (2θ) was 5–90° with step size of 0.050° and counting time of 2 s/step. Quartz was used as the standard material to accurate for the instrumental expansion. This identification of the complexes was done by a known method. From the fit identified Scherer formula, the average crystallite size (D) is $D = (K\lambda/\beta \cos \theta)$ Where: λ is the X-ray wavelength in the nanometer, K is factor related to crystallite shape, and with a value about 0.9 and β is the peak width at half maximum height. The value of β in the 2θ axis of diffraction shape must be in radians. The θ is the Bragg angle and be able to in radians since the $\cos \theta$ compatible with the same number.

2.5 Computational Studies

The input files of ligand and its metal complexes were prepared with Gauss View 5.0.8. Gaussian 09 rev. A.02 [13] was used to make the all calculations by the DFT/B3LYP method. 6-31G and LANL2DZ are the standard basis sets for the synthesized ligand and its metal complexes, respectively.

2.6 Irradiation Studies

For irradiation studies of solid samples of ligand and complexes were subjected to γ -irradiation [14] to a dose of 60 kGy using Indian 60 Co γ -ray cell type GE-4000 A (at room temperature at the Egyptian Atomic Energy Authority Nasr City, Egypt) at a dose rate of 2.2 kGy h^{-1} . After removing the samples from the radiation field the FT-IR, absorption spectra, XRD and thermal analysis (TG/DTG) and biological activity of the irradiated samples were investigated by the same methods used for before irradiated compound.

2.7 Antibacterial Activity

The in vitro antibacterial activity studies were carried out at Genetic Engineering and Biotechnology Research Institute, Department of Environmental Biotechnology at Sadat City University, Egypt, by using Broth Dilution Method [15] with some alterations, to investigate the inhibitory effect of some synthesized complexes before (B_1 – B_4) and after

(A_1 – A_4) irradiation on the sensitive organisms *Streptococcus pyogenes* as for Gram-positive bacteria and *Escherichia coli* as Gram-negative bacteria. Nutrient broth medium and Brain Heart Infusion (BHI) medium were used as cultivation media for *Escherichia coli* and *Streptococcus pyogenes*, respectively. The test compounds in measured quantities were dissolved in DMSO which has no inhibition activity to get two different concentrations (1, 5 and 10 mg/mL) of compounds. The strains selected for the study were prepared in nutrient broth and (BHI) broth medium with shaking and autoclaved for 20 min 15 pounds of pressure and at 121 °C before inoculation. The bacteria were then cultured for 24 h at 37 °C in an incubator. One ml of the standard bacterial culture was used as inoculation volume. For growth studies, culture of microbial cells was inoculated and grown aerobically in nutrient broth and BHI broth for control and along with various concentrations of the test compounds in individual flasks. Growth was calculated turbidometrically at 650 nm using conventional Spectrophotometer, in which turbidity produced is measured by taking absorbance and compared with turbidity produced by control. The growth rate of different bacteria in the absence as well as in the presence of test compounds was performed for each concentration. Absorption measurements were accomplished by spectrophotometer after 24 and 48 h of incubation to determine the number of viable cells per milliliter of sample and were used to the calculated the % inhibition.

2.8 Molecular Docking

All docking steps were done by MOE 2008 (Molecular Operating Environment) software [16] to simulate the binding model of these compounds into topoisomerase II DNA gyrase enzymes (2XCT). The protein crystal structure was obtained from the Protein Data Bank (PDB).

3 Results and Discussion

3.1 Elemental Analysis and Molar Conductance

The analytical and physical data of the prepared ligand and metal complexes are collected in Table 1. The chemical composition and stoichiometry of the prepared metal complexes were confirmed by the results of analytical and spectral tools. The obtained data showed satisfactory agreement with the proposed molecular formulae. These data also indicated that the metal complexes have 1:1 (metal/ligand) (B_1 and B_4) or 1:2 stoichiometry for complexes (B_2 and B_3).

The complexes are found to be air stable for a long time, insoluble in different organic solvents such as (ethanol, methanol, carbon tetrachloride, chloroform, dichloromethane and acetone) but soluble to great extent



Table 1 Elemental analyses and physical properties of ligand(B) and its metal complexes

No	Molecular formula	(Empirical formulae)	M.wt	Color (yield %)	C	H	N	M	Λ_m
B	H ₂ L	(C ₁₆ H ₁₈ N ₄ OS)	314	Buff 75	61.1 (61.3)	5.73 (5.70)	17.8 (17.9)	–	–
B ₁	Cu(H ₂ L)I	(C ₁₆ H ₁₈ N ₄ OSICu)	504.5	Green 78	38.1 (38.4)	3.6 (4.2)	11.1 (11.4)	12.6 (12.3)	25
B ₂	Cu(H ₂ L) ₂ (ClO ₄) ₂	(C ₃₂ H ₃₆ N ₈ O ₁₀ S ₂ Cl ₂ Cu)	889.5	Green 60	43.2 (43.8)	4.0 (3.78)	12.6 (12.9)	7.1 – (7.6)	24
B ₃	[Zn (H ₂ L) ₂ (H ₂ O)]SO ₄	(C ₃₂ H ₃₈ N ₈ O ₇ S ₂ Zn)	807.4	Yellow 65	47.5 (47.2)	4.7 (4.9)	13.8 (13.6)	8.1 (8.3)	72
B ₄	[Cd (H ₂ L)Cl]Cl	(C ₁₆ H ₁₈ N ₄ OSCl ₂ Cd)	497.4	White 70	38.6 (39.2)	3.6 (4.3)	11.3 (11.5)	22.6 (23.0)	65

Λ_m = molar conductivity (ohm⁻¹ cm² mol⁻¹) in 10⁻³ M DMF solution

in DMF and DMSO. Conductivity measurements in non-aqueous solution have frequently been used in structural studies of the prepared metal complexes within the limits of their solubility. The molar conductance values of 10⁻³ M solution of the complexes in DMF that are listed in Table 1 show that copper complexes (B₁ and B₂) are non-electrolytes [17, 18]. However, complexes (B₃, B₄) show molar conductivity values of 72 and 65 Ω⁻¹ cm² mol⁻¹ indicating 1:2 and 1:1 electrolyte, respectively [19, 20].

3.2 Nuclear Magnetic Resonance Spectroscopy

Comparison of the proton nuclear magnetic resonance of *N*-phenyl-2-(*p*-tolylglycyl)hydrazine-1-carbothioamide (B) ligand before and after γ - irradiation (B and A) recorded in DMSO-*d*₆ solution is shown in Figure S1. The ¹H NMR spectrum of the ligand before γ —irradiation(B) in DMSO-*d*₆ exhibited a chemical shift (δ /ppm), before and after γ - irradiation, the N(4)H signal appears at 9.44 ppm and the N(2)H signal appears at 9.51, 10.05 ppm indicating the involvement of these hydrogen through intra-molecular hydrogen bonding with the carbonyl oxygen, the peak of N(1)H appeared at 9.62 ppm for ligand after gamma irradiation. The singlet signal appears at 2.14, 3.9, 3.7 ppm attributed to the protons of methyl CH₃, singlet signal appears at 3.7 ppm attributed to the protons of CH₂, the multiplet signal appears at 5.85–7.1, 6.5–7.4 ppm attributed to the aryl protons. The intensity of the bands after irradiation is higher than before irradiation, and some bands disappear upon irradiation [21]. Also, ¹H NMR spectra of [Zn(H₂L)₂]SO₄ before and after γ -irradiation (B₃,A₃) displayed signals at 2.14(s, 6H, 2CH₃), 3.76(s,4H,2CH₂), 5.59(s,2H,2NH), 6.32–7.43(m, 18H, Ar–H), 9.55(s,1H, NH) and 10.51(s, H, NH) as shown in Fig. 1 and. While [Cd(H₂L)Cl] Cl before and after γ -irradiation (B₄, A₄) complexes displayed signals at 2.16(s, H, CH₃), 3.77(s,2H,2CH₂), 5.56(s, H, NH),

6.51–7.52(m, 9H, Ar–H), 9.44 (s,1H, NH), 9.61 (s,1H, NH) and 10.05(s, H, NH) as shown in Figure S2.

The effect of γ -irradiation on the chemical shift of [Zn(H₂L)₂]SO₄ and [Cd(H₂L)Cl]Cl after γ -irradiation is insignificant.

3.3 Mass Spectroscopy

Mass spectrum confirms the structure of the ligand as indicated by the molecular ion peak (M⁺) corresponding to its molecular weight Figure S3. MS of B, the observed peak at $m/z = 313$ corresponding to (C₁₆H₁₈N₄OS, atomic mass $m/z = 314$ molecular ion peak). The spectrum also shows important fragment ions in the range $m/z = 51$ for [C₄H₄–H]⁺, 77 for [C₆H₅]⁺, 107 for [C₇H₈N]⁺ base peak, 120 for [C₇H₆NO]⁺, 135 for [C₈H₇S]⁺ and 280 for [C₁₄H₁₃N₃SO–H]⁺

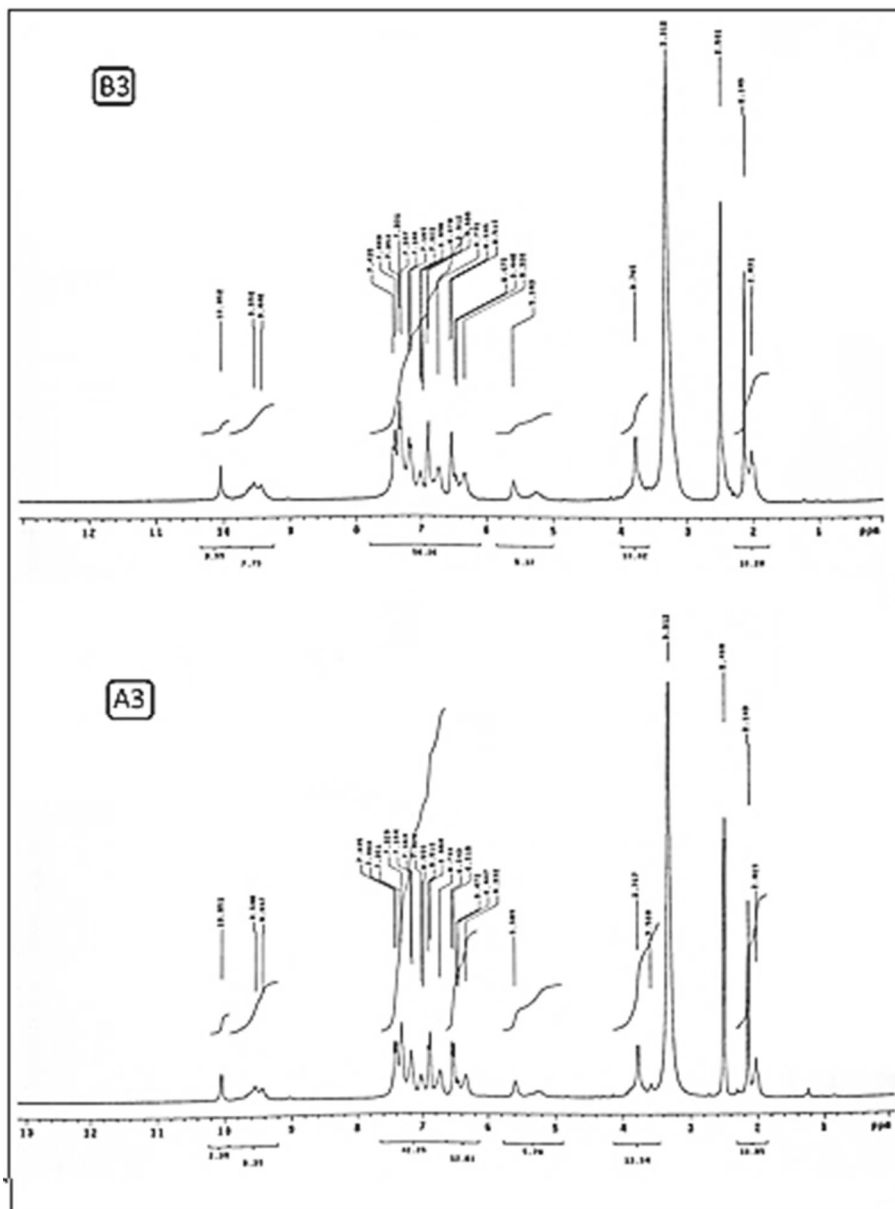
Also, the mass spectrum of complex (B₃) confirms its proposed formula by showing a molecular ion peak at m/z 807.4 amu corresponding to [Zn(H₂L)₂(H₂O)]SO₄ (B₃) Figure S4 which coincide with its formula weight (calculated $m/z = 807.4$ amu). The other fragments of the complex give the peak with various intensities at different m/z values like at Calc/Found: 77[C₆H₅], 91[C₆H₄NH], 120[C₉H₈NH], 255[C₁₃H₁₃N₅O], 535[C₂₄H₂₄N₈O₂], 715[C₃₀H₂₉N₈O₄S₂], 783[C₃₀H₃₈N₈O₇S₂Zn], 807.4/806 [C₃₂H₃₈N₈O₇S₂ Zn].

3.4 FT-IR Spectra

3.4.1 FT- IR Spectra of the Ligand Before and After γ -Irradiation

Gamma irradiation can change the properties and morphology of matter and that exhibit in physical techniques as FT-IR, and the following comparison between the functional

Fig. 1 ¹H NMR spectra of complexes B₃ before and after irradiation A₃ in DMSO-d₆ solution



groups of the ligand before and after irradiation (B and A) is presented in Fig. 2 and Table 2. It has been found that the functional groups of the ligand before γ -irradiation and after presented at 3384,3336 cm^{-1} ; 3263,3185 cm^{-1} ; 3150,3126 cm^{-1} ; 1672,1689 cm^{-1} and 749,750 cm^{-1} are attributed to the stretching frequencies of $\nu(\text{N4-H})$, $\nu(\text{N2-H})$ and $\nu(\text{N1-H})$, $\nu(\text{C=O})$ and $\nu(\text{C=S})$, respectively. After γ -irradiation, the bands corresponding to $\nu(\text{C=O})$ slightly shift to higher frequencies as compared with before γ -irradiation [6]. After γ -irradiation, the peaks are sharper than before γ -irradiation, where we notice a change in frequency and intensity of peak we also note this change also in complexes.

Where: B = before γ -irradiation, A = after γ -irradiation.

3.4.2 FT-IR Spectra of Copper Complexes Before and After γ -Irradiation

The FT-IR spectra of the Cu(I), Cu(II) complexes before and after γ -irradiation (B₁, B₂ and A₁, A₂) show significant changes compared to the spectrum of their free ligand Figs. 3 and S5. The most important diagnostic spectral bands are summarized in Table 2. The IR spectra of copper complexes (B₁ and B₂) show strong bands at 3431, 3437; 3293, 3295; 1597, 1595 and 740, 754 cm^{-1} for before irradiation and at 3434, 3433; 3295; 3297; 1597; 1595 and 745,756 cm^{-1} for (A₁ and A₂) after irradiation which assigned to the stretching frequencies of $\nu(\text{N4-H})$, $\nu(\text{N2-H})$, $\nu(\text{C=O})$ and $\nu(\text{C=S})$, respectively. The IR spectra of copper complexes before

Fig. 2 IR spectra of the ligand (B) before irradiation and after irradiation (A)

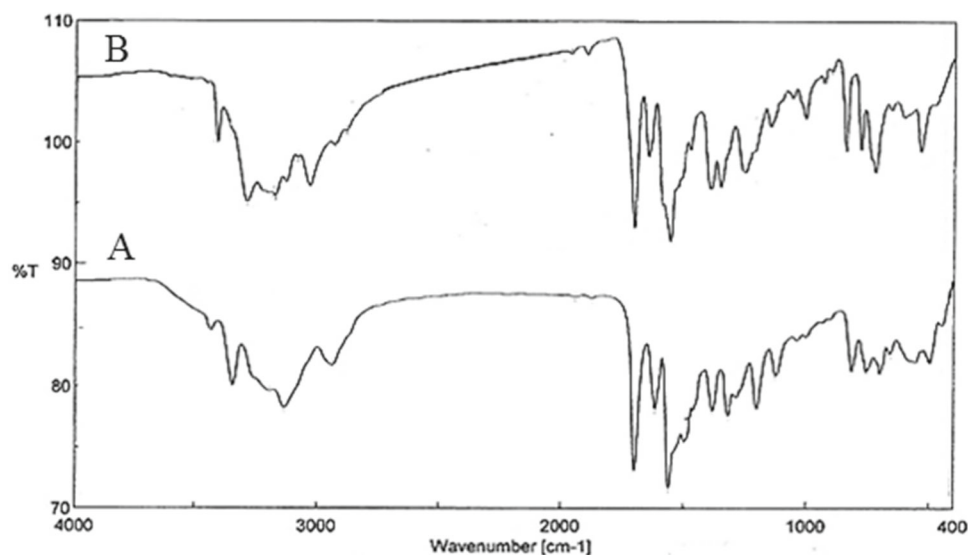


Table 2 Infrared spectral bands (cm^{-1}) for ligand and its metal complexes before and after irradiation

No	Compound	$\nu(\text{OH})/\nu(\text{N4-H})$	$\nu(\text{N2-H})$	$\nu(\text{N1-H})$	$\nu(\text{C=O})$	$\nu(\text{C=S})$	$\nu(\text{M-O})$	$\nu(\text{M-N})$
B	H_2L	3384	3263	3150	1672	749	—	—
A	H_2L	3336	3185	3126	1689	750		
B ₁	$\text{Cu}(\text{H}_2\text{L})\text{I}$	3431	3293	3183	1597	749	603	529
A ₁	$\text{Cu}(\text{H}_2\text{L})\text{I}$	3434	3295	3185	1597	750	602	529
B ₂	$\text{Cu}(\text{H}_2\text{L})_2(\text{ClO}_4)_2$	3437	3295	3153	1595	754	614	545
A ₂	$\text{Cu}(\text{H}_2\text{L})_2(\text{ClO}_4)_2$	3433	3297	3154	1595	756	612	539
B ₃	$[\text{Zn}(\text{H}_2\text{L})_2(\text{H}_2\text{O})]\text{SO}_4$	3420	—	3170	1593	754	614	512
A ₃	$[\text{Zn}(\text{H}_2\text{L})_2(\text{H}_2\text{O})]\text{SO}_4$	3420	—	3138	1619	755	618	512
B ₄	$[\text{Cd}(\text{H}_2\text{L})\text{Cl}]\text{Cl}$	3426	3268	3179	1685	744	591	533
A ₄	$[\text{Cd}(\text{H}_2\text{L}_A)\text{Cl}]\text{Cl}$	3433	3269	3179	1685	744	591	532

irradiation show that $\nu(\text{C=O})$ and $\nu(\text{N2-H})$ shift to lower frequency upon complexation as compared of free ligand, indicating the coordination of the ligand in keto-form and the ligand behaves as neutral bidentate or tridentate, coordination take place via (C=O) and $\text{N}(2)\text{H}$ (B_2) and (C=S) (B_1).

The IR spectra of Cu(I), Cu(II) complexes before and after γ -irradiation display new bands at 603, 614 and $529, 545 \text{ cm}^{-1}$ assigned to $\nu(\text{Cu-O})$ and $\nu(\text{Cu-N})$, respectively [22, 23]. New bands appear at 1109, 1113 cm^{-1} assigned to $\nu(\text{ClO}_4)$. IR spectra of the complexes (A_1 and

A_2) showed that the intensity of the IR bands became sharper than after γ -irradiation [24].

3.4.3 FT-IR Spectra of Zinc(II) Complexes Before and After γ -Irradiation

The IR spectra of Zn(II) complexes Figure S6 show strong bands at 3420, 3170, 3164, 1593, 1619 and $738, 743 \text{ cm}^{-1}$ before irradiation and after γ -irradiation which attributed to the stretching frequencies of $\nu(\text{N4-H})$, $\nu(\text{N1-H})$, $\nu(\text{N2-H})$, $\nu(\text{C=O})$ and $\nu(\text{C=S})$ wagging vibrations, respectively. In the

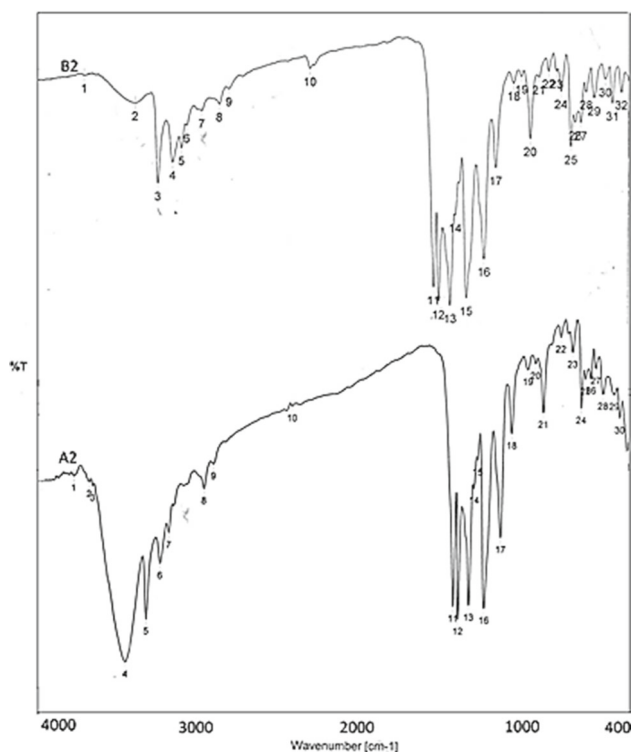


Fig. 3 IR spectra of copper(II) complexes before irradiation (B₂) and after irradiation (A₂)

IR spectra of Zn(II) complex before and after γ -irradiation, it is seen that the band corresponding to $\nu(\text{C}=\text{O})$ was shifted to lower frequency upon complexation and the ligand behaves as neutral bi/tridentate and coordination takes place via (C=O), (N₂-H) and (C=S). High intensity of the function groups bands was observed after γ -irradiation. The new bands appeared at 614, 618 and 512 cm^{-1} are assigned to $\nu(\text{Zn}-\text{O})$ and $\nu(\text{Zn}-\text{N})$, respectively [25]. New bands at 1027, 1025 cm^{-1} display $\nu(\text{SO}_4)$ for complexes (B₃ and A₃).

3.4.4 FT-IR Spectra of Cd(II) Complexes Before and After γ -Irradiation

The FT-IR spectra of Cd(II) complexes Fig. 4 show strong bands at 3426, 3433; 3268, 3269; 3179; (1675, 1613, 1617) and 735 cm^{-1} for before irradiation and after γ -irradiation which attributed to the stretching frequencies of $\nu(\text{N}_4-\text{H})$, $\nu(\text{N}_2-\text{H})$, $\nu(\text{N}_1-\text{H})$ and $\nu(\text{C}=\text{S})$ wagging vibrations, respectively. The IR spectra of Cd(II) complexes before and after γ -irradiation showed that the band corresponding to $\nu(\text{C}=\text{O})$ is shifted to higher frequency upon complex formation and the ligand behave as neutral tridentate and coordination take place via (C=O), (N₂-H) and (C=S). The new bands appeared at 591, 533 and 532 cm^{-1} assigned to $\nu(\text{Cd}-\text{O})$ and $\nu(\text{Cd}-\text{N})$, respectively [26].

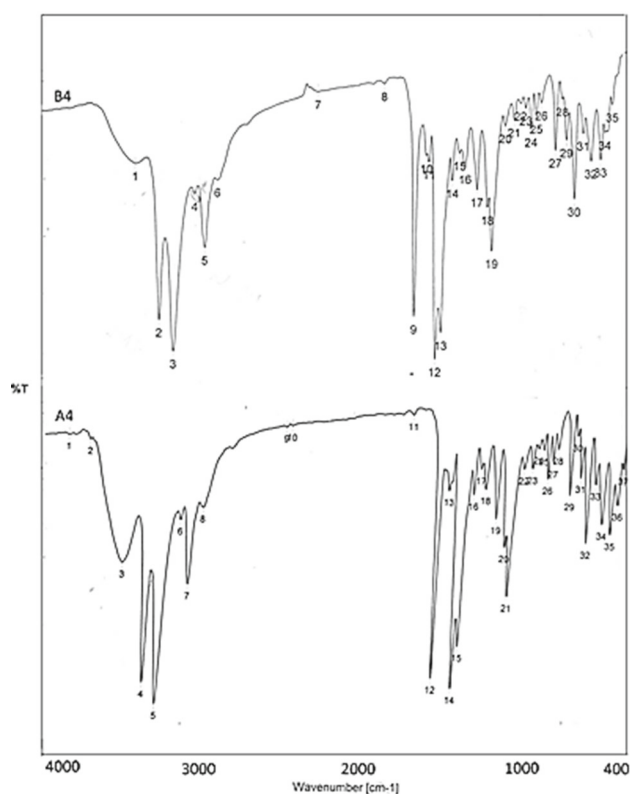


Fig. 4 IR spectra of Cadmium complexes before irradiation (B₄) and after irradiation (A₄)

3.5 UV-Vis Spectra and Magnetic Moment Properties

The electronic spectral data of the ligand (B) and Cu(I), Cu(II), Zn(II) and Cd(II) complexes in DMF solution within the range 200–800 nm are tabulated in Table 3 and depicted in Figures S7–S10. The electronic spectrum of the ligand exhibits bands at 314, 292 and 279 nm, respectively.

3.5.1 The Electronic Absorption Spectra of Copper Complexes Before and After γ -Irradiation

The electronic spectra of Cu(I) complexes Figure S₅ before and after irradiation (B₁ and A₁) displayed bands at 300 and 409 nm, respectively. Cu(I) ions have the d^{10} configuration, and therefore, the Cu(I) complexes should not exhibit any d-d transition and have tetrahedral geometry [27].

While the electronic absorption spectra of Cu(II) (B₂ and A₂) Figure S₈ before and after irradiation exhibited bands at 308, 398 and 653 nm in DMF refer to L \rightarrow M charge transfer and d \rightarrow d transitions, respectively, in an octahedral geometry [28]. Diamagnetic behavior of complex (B₁) and the magnetic suitability value of complexes (B₂, A₂) 1.8 B.M. are an indicative of tetrahedral and octahedral geometry [27, 29].

Table 3 The electronic absorption spectral data in DMF solution of ligand and its magnetic moment and its metal complexes before and after irradiation value

No	Compound	Assignment		
		DMF	μ_{eff} (B.M.)	Geometry
B	H ₂ L	314, 292, 279	–	L
B ₁	Cu(H ₂ L)I	300	Dia.	Tetrahedral
		409		
A ₁	Cu(H ₂ L)I	300	Dia.	Tetrahedral
		408		
B ₂	Cu(H ₂ L) ₂ (ClO ₄) ₂	653	1.74	Octahedral
		398		
		308		
A ₂	Cu(H ₂ L) ₂ (ClO ₄) ₂	653	1.74	Octahedral
		398		
		308		
B ₃	[Zn (H ₂ L) ₂ (H ₂ O)]SO ₄	448	Dia.	Octahedral
		300		
A ₃	[Zn (H ₂ L) ₂ (H ₂ O)]SO ₄	445	Dia.	Octahedral
		282		
B ₄	[Cd (H ₂ L)Cl]Cl	610	Dia.	Tetrahedral
		390		
		284		
A ₄	[Cd (H ₂ L)Cl]Cl	608	Dia.	Tetrahedral
		385		
		282		

3.5.2 Zinc(II) Complexes Before and After γ -Irradiation

The electronic absorption spectra of Zn(II) complexes Figure S9 before and after γ -irradiation displayed bands at 300, 282; 448 and nm in DMF solution, octahedral structure of Zn(II) complex is suggested which is diamagnetic in nature [30].

3.5.3 Cadmium(II) Complexes Before and After γ -Irradiation

The electronic absorption spectra of Cd(II) complexes Figure S10 before and after γ -irradiation displayed three bands at 284, 390, 610 nm; 282, 385 and 608 nm in DMF solution attributed to charge transfer transition which assigned to tetrahedral geometry around Cd(II) ion [31, 32]. The Cd(II) complexes are diamagnetic because of d^{10} electronic configuration of Cd(II) ion [33].

3.6 X-ray Diffraction Patterns

XRD analysis was performed to confirm the crystal phase of compound. Samples (B₁, B₂, A₂ and B₃, A₃) for before and after irradiation as shown in Figures S11–S13 and Table 4. The XRD patterns of the synthesized compounds were carried out in order to give an insight about the lattice dynamics

of the compounds. The X-ray diffraction was recorded by using (CuK α) radiation (1.5406 Å). The intensity were collected over a 2θ range of 5–90°. The average grain size of the samples was estimated using the diffraction intensity peak. The mean grain size (D) of the particles was determined from the XRD line broadening measurement using the Scherrer equation [18, 34, 35]: $D = 0.89\lambda/\beta (\text{Cos}\theta)$.

An observable peak sharpness in the diffraction pattern indicates that the Cu(I), Cu(II) and Zn(II) complexes before and after irradiation Figures S11–S13 and Table 4 are in the nanometer range. The diameter of particles is found in nanorange scale as follows: Cu(I) complex before (B₁) 4.83 nm; Cu(II) complexes before and after irradiation (B₂ and A₂) 3.6, 5.79 nm; Zn(II) complexes before and after irradiation (B₃ and A₃) 5.97, 3.84 nm. The nanoparticles sized complexes may serve strongly in different application fields in between the biological one [36, 37]. Figures S11–S13 show that in Cu(I), Cu(II) and Zn(II) complexes new peaks appear and some peaks displaced to longer interplanar spacing. The major factors tending to influence the intensity of powder patterns are structure factor, polarization factor, atomic scattering factor, multiplicities and preferred orientations. Upon irradiation, the position of atoms in the lattice changes and consequently, the scattering power also changes, leading to

Table 4 XRD data of Cu(I), Cu(II) and Zn(II) complexes before (B₁, B₂, B₃) and after irradiation(A₂,A₃)

	B ₁	B ₂	B ₃	A ₂	A ₃	
Angle 2θ	8.2714	5.4796	6.6762	8.2002	6.6293	
	21.1130	6.6475	11.1930	23.6566	12.0777	
	23.6719	8.7388	12.1177	25.3683	13.4246	
	25.3735	21.9376	13.4750	28.2666	19.1065	
	42.0811	23.5451	19.1602	42.0890	20.0901	
	49.08440	26.7430	20.1275	49.8356	21.01650	
	d- value Å	10.68097	16.11496	13.22906	10.77355	13.32254
		4.20458	13.28611	7.89872	3.75794	7.32205
		3.75554	10.11071	7.29797	3.50812	6.59030
		3.50741	4.04836	6.56576	3.15466	4.64136
2.14551		3.77548	4.62848	2.14513	4.41629	
1.82802		3.33083	4.40817	1.82831	4.19437	
FWHM	0.36400	0.32540	0.23340	0.29380	0.36300	
	0.42670	0.39730	0.24200	0.40670	0.23540	
	0.34640	0.38950	0.26890	0.26470	0.26640	
	0.31710	0.81600	0.24240	0.29330	0.23490	
	0.28810	0.52750	0.22050	0.24600	0.26420	
	0.31140	0.4900	0.26500	0.21410	0.21000	
Grain size nm	3.84	4.27	5.97	4.75	3.84	
	3.47	3.51	5.83	3.71	6.02	
	4.36	3.6	5.27	5.79	5.34	
	4.83	1.83	5.87	5.36	6.24	
	6.47	2.86	6.65	7.59	5.58	
	6.78	3.16	5.57	10.03	7.07	

changes in intensity which displays high resistance [38]. It should be noted that the Zn(II) complex (A₃) after irradiation showed increase in the crystalline size than B₃ before irradiation.

3.7 Thermal Behavior of Ligand and Metal Complexes Before and After γ -Irradiation

The thermal behavior of the ligand and Cu(I), Cu(II), Zn(II) and Cd(II) complexes before and after γ -irradiation was investigated by thermogravimetric technique in temperature range 25–800 °C. The thermal behavior data of the ligand and Cu(I,II), Zn(II) and Cd(II) complexes (B₁–B₄ and A₁–A₄) before and after γ -irradiation are tabulated in Table 5 and depicted in Figs. 5 and S14 and S15.

3.7.1 The Ligand Before and After γ -Irradiation

The TG curves of the ligand before and after γ -irradiation show that it is thermally stable till 140 °C, and 125 °C, respectively. Also, the TG curves show three decomposition steps in the temperature range 140–550 °C; 125–510 °C with total

weight loss of Calc.100% (Found 100%) before and after γ -irradiation, respectively.

3.7.2 Copper Complexes

The TG thermograms of complexes (B₁ and A₁) display three steps of decomposition as shown in Table 5 and Fig. 5. The first step of decomposition appeared within the temperature range 134–255 and 147–293 °C with mass loss of 21% (calc. 21.2%) and 28.7% (calc. 28.3%) for complex (B₁) and complex (A₁), respectively, corresponding to loss of (CH₃C₆H₅NH) and (HI + NH). The second step appeared at 258–410 and 294–385 °C with mass loss of 19.0% (calc. 18.2%) and 11.0% (calc. 10.1%) for complexes (B₁ and A₁), respectively, corresponding to further decompositions of organic ligand. The third TG decomposition step appeared within the temperature ranges 410–753 °C and 385–701 °C with mass loss of 36.0% (calc. 36.5%) and 35.0% (calc.34.1%), respectively, corresponding to complete decomposition of the organic ligand. The final remained product appeared above 735 °C with remain mass of 24.0% (calc. 22.9%) for complex (B₁) and above 701 °C with mass

Table 5 Thermal analysis data of ligand and Cu(I), Cu(II), Zn(II) and Cd(II) complexes before and after irradiation

No	Molecular formulae	Temp. range (°C) DTG	Temp. range (°C) TGA	Mass loss %		Assignment
				Found	Calc.	
B	H ₂ L	180,500	140 140–550	– 100	– 100	Melting decomposition
A	H ₂ L	180,550	125 125–510	– 100	– 100	Melting decomposition
B ₁	Cu(H ₂ L)I	206 313 639	134–255 255–410 410–753	21 19.0 36.0	21.2 18.2 36.5	Loss of CH ₃ C ₆ H ₅ NH Further decomposition Completion of decomposition of organic ligand
A ₁	Cu(H ₂ L)I	287 314 602	147–293 294–385 385–701	28.7 11 35	28.3 10.1 34.1	CuO + 3C Loss of CH ₃ C ₆ H ₅ NH + HI + NH Further decomposition Complete decomposition of organic ligand
B ₂	Cu(H ₂ L) ₂ (ClO ₄) ₂	547, 637, 685	420–620 At 620	82 18	83 17	Decomposition CuO + 7C as final product
A ₂	Cu(H ₂ L) ₂ (ClO ₄) ₂	429	440–790 At 790	84.4 15.6	84.3 15.7	Decomposition CuO + 6C as final product
B ₃	[Zn(H ₂ L) ₂ (H ₂ O)] SO ₄	216 384	180–332 332–499	39 39	39.3 38.8	Decomposition Complete decomposition of the organic ligand
A ₃	[Zn(H ₂ L) ₂ (H ₂ O)] SO ₄	646 220 599	499–704 170–374 374–660	22 50 29	21 50.3 28	ZnO ₂ + 7C Decomposition Complete decomposition of the organic ligand
B ₄	[Cd (H ₂ L)Cl]Cl	186 257	134–789 At 789	88.2 11.8	88.4 11.6	Decomposition Complete decomposition of the organic ligand
		335 701				Cd
A ₄	[Cd (H ₂ L)Cl]Cl	186 331 644	139–718 At 718	82.7 17.3	82.3 46.6	Decomposition Complete decomposition process
					17.7	CdO + 2C

remain of 25.3% (calc. 25.3%) for complex(A₁) represent the formation of (CuO + 3C) and (CuO + 4C) as a final product [39].

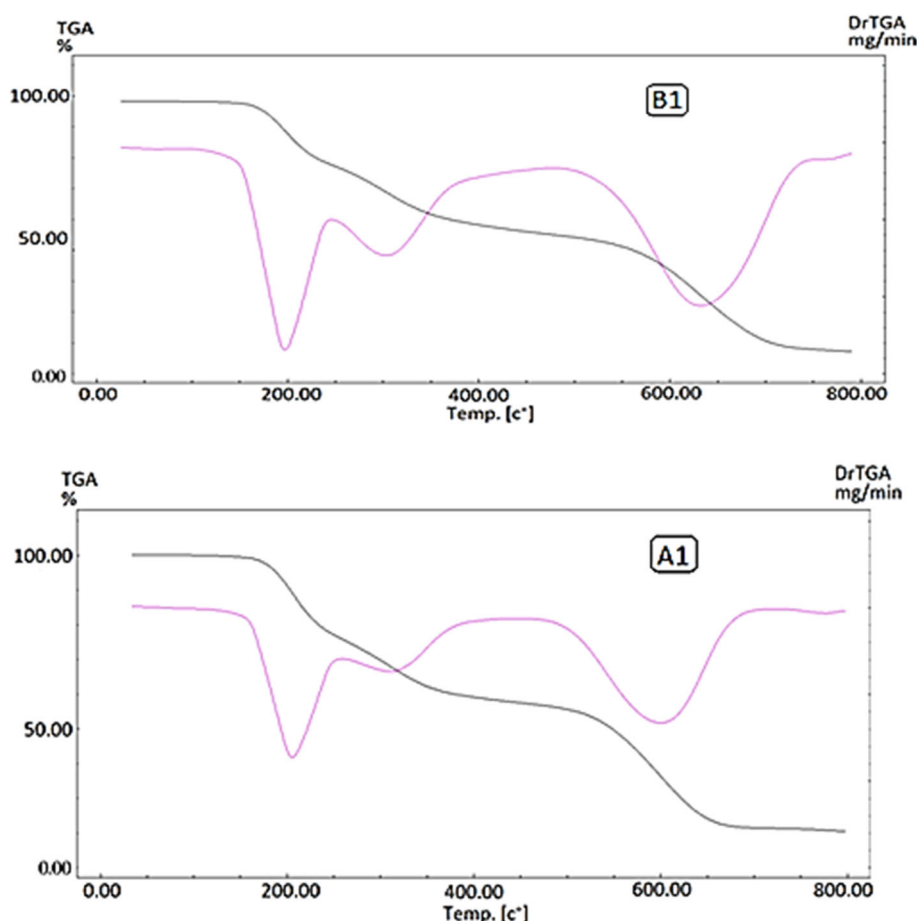
The TGA curve of complexes (B₂ and A₂) displays successive steps of decomposition as shown in Table 5. The decomposition starts within the temperature range 420–620 and 440–790 °C with mass loss of 82.0% (calc. 83%) and 84.4% (calc. 84.6%) for complex (B₂) and complex (A₂), respectively. The final thermo-product appeared at 620 °C with mass loss 18.0% (calc. 17%) for complex (B₂) and at 790 °C with mass loss 15.6% (calc. 15.7%) for complex(A₂)

represents the formation of (CuO + 7C) and (CuO + 6 C) as a final product [39].

3.7.3 Zinc (II) Complex

The TG thermograms of complexes (B₃, A₃) Figure S14 showed several steps of decomposition. The first step of decomposition appeared at 180–332 and 170–354 °C with mass loss 39% (calc. 39.3%) and 50% (calc. 50.3%) for complexes B₃ and A₃ which corresponded to decomposition of organic ligand. The second step of decomposition appeared at

Fig. 5 TGA/ DTG curves of complexes before irradiation (B₁), after irradiation (A₁)



332–749 and 354–705 °C with mass loss 39% (calc. 38.8%) and 50% (Calc.50%), respectively, for complexes (B₃, A₃) which attributed to complete decomposition of organic ligand. The remaining weight for complex (B₃) appeared above 704 °C and above 660 °C with mass remain of 22.1% (calc. 21%) and 21% (calc. 21.7%) corresponding to the formation of ZnO as final products in addition to 7C residue [39].

3.7.4 Cadmium (II) Complexes

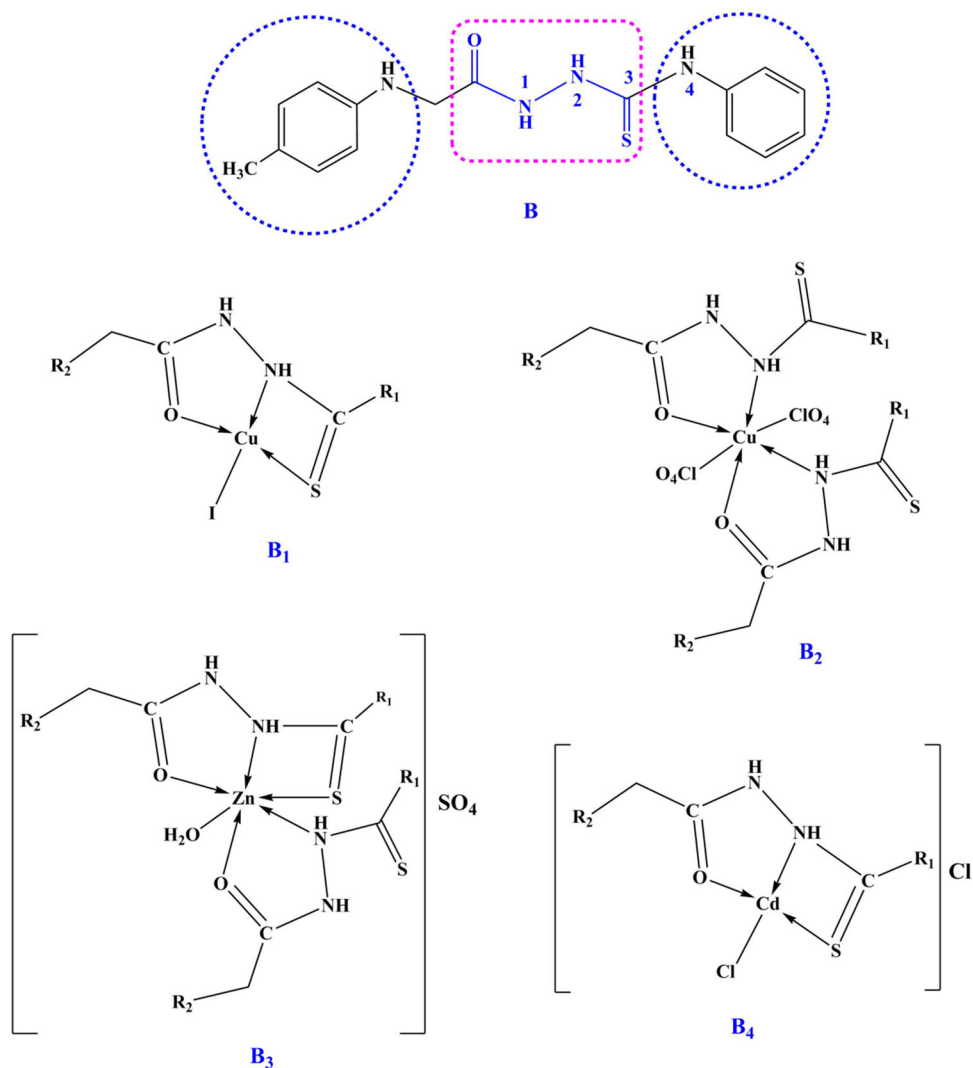
The TG thermograms of complexes (B₄, A₄) Figure S15 display successive decomposition steps within the temperature range 134–789 and 139–718 °C with mass loss 88.2% (calc. 88.5%), respectively, for complexes (B₄, A₄), are assigned to the material decomposition. The final weight residue appeared at above 789 and 718 °C corresponded to Cd and CdO for complexes (B₄, A₄) as thermo-final products in addition to carbon residue for complex (A₄) [24, 40] (Fig. 6).

From the above assignment, the suggested chemical structure of the ligand and Cu(I),Cu(II), Zn(II) and Cd(II) complexes(B₁–B₄) is shown in Fig. 5

3.8 Structure Characterization with DFT Study

The geometric structures of H₂L ligand and its metal complexes were optimized as shown in Fig. 7. Upon coordination of H₂L to the metal atom, some bond lengths become slightly longer than in the free ligand accompanied with changes in angles that are clarified in Table 6 as (C5–O8), (N4–C5), (N7–C6) and (N3–C2). This finding is due to the formation of M–N & M–O bonds in all complexes that make the C–O [41, 42] and C–N bonds weaker [43]. It was observed from the energy values that the stability of ligand increases upon complexation with Zn (II) and Cu(II) ions in ratio (1–2) metal to ligand. The ionic complexes (Cd(II) & Cu(I)) show higher energy values than the parent ligand. The polarity of ligand increased after complexation by its coordination to metal ions as it is evident from the magnitude of their dipole moments. The ionic complexes have higher polarity than the non-electrolytic complexes. The molecular properties are mentioned in Table 6 which can be calculated as follows: Hardness $\eta = (I - A)/2$, Softness (S) $S = 1/2\eta$, Chemical potential (μ), $\mu = -(I + A)/2$ and Electronegativity (χ), $\chi = (I + A)/2\eta$. From HOMO–LUMO gap (ΔE), one can detect whether the molecule is hard or soft. Larger ΔE

Fig. 6 The suggested chemical structures of the ligand and its metal complexes



Complexes	R ₁	R ₂
B ₁ , B ₂ , B ₃ , B ₄	C ₆ H ₅ NH-	CH ₃ C ₆ H ₄ NH-

corresponding to harder molecule and small one related to the softer molecule. The polarizability of the soft molecule is more than the hard one because it needs lower energy to excitation, thus softness (S) and hardness (η) are properties of molecule that measures the chemical reactivity. We found the ligand and Cu(I) complex were more harder than the remaining complexes. The generated molecular orbital energy diagrams HOMO and LUMO are presented in Fig. 8.

The formal charge of cadmium, zinc and copper was Cd²⁺, Zn²⁺, Cu²⁺, Cu⁺, but the calculated charges on [Cd(H₂L)Cl]Cl, Cu(H₂L)₂(ClO₄)₂, Cu(H₂L)I and [Zn(H₂L)₂(H₂O)] SO₄ were 0.856, 0.579, 0.413 and 0.884, respectively. It can be explained due to the charge

transfer from the examined ligand to the central metal ions, i.e., L → M. So, the theoretical calculations confirm the results that obtained from the analysis tools which were discussed in the previous characterization part (Table 7).

3.9 Antibacterial Activity

The utilization of heavy metal compounds as a choice to treat bacterial borne diseases shows up as a novel and promising thought. A few reports affirm the antimicrobial capability of copper and zinc compounds on different microbes that cause nosocomial illness in people [44–46]. Our results showed an attempt to use metals complexes as an alternative choice in

Fig. 7 Optimized 3D structures of ligand **a** H₂L(B), **b** [Cu(H₂L)I](B₁), **c** [Cu(H₂L)₂ClO₄](B₂), **d** [Zn(H₂L)₂(H₂O)]SO₄(B₃) and **e** [Cd(H₂L)Cl]Cl (B₄)

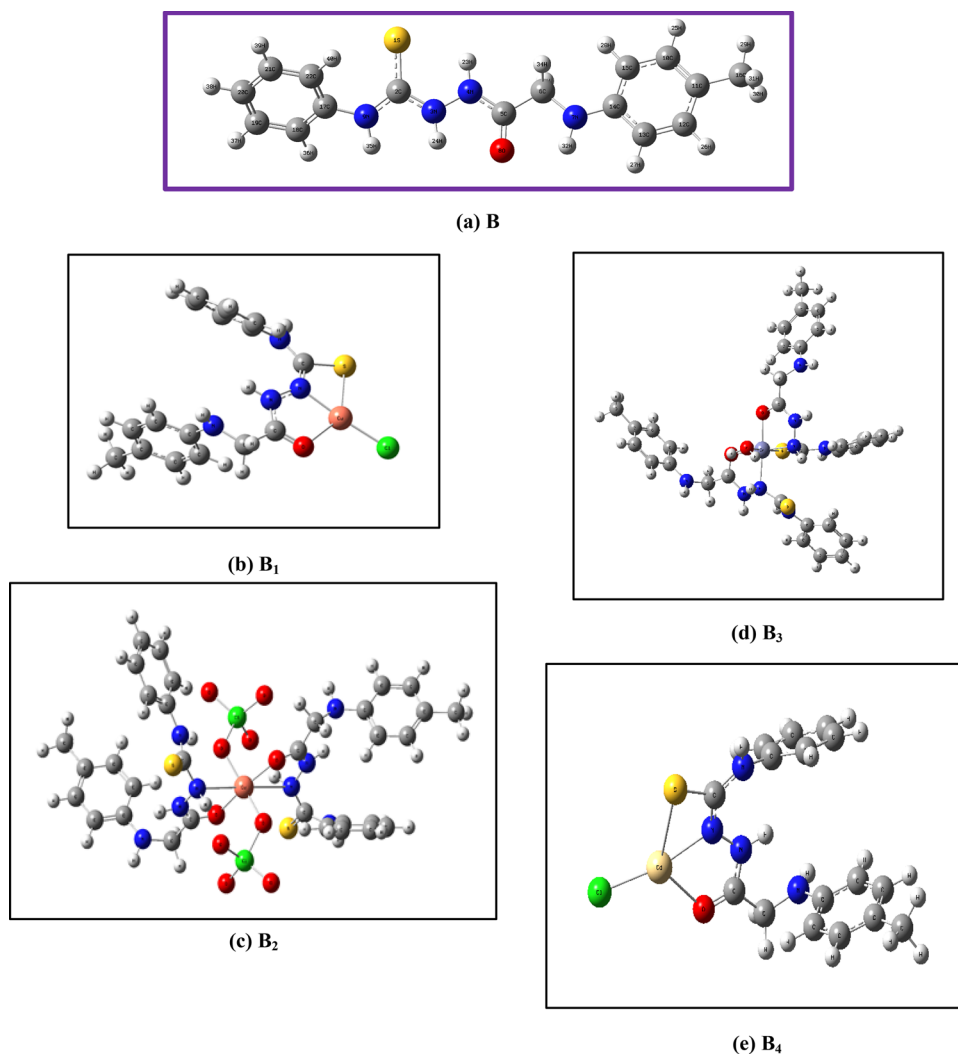
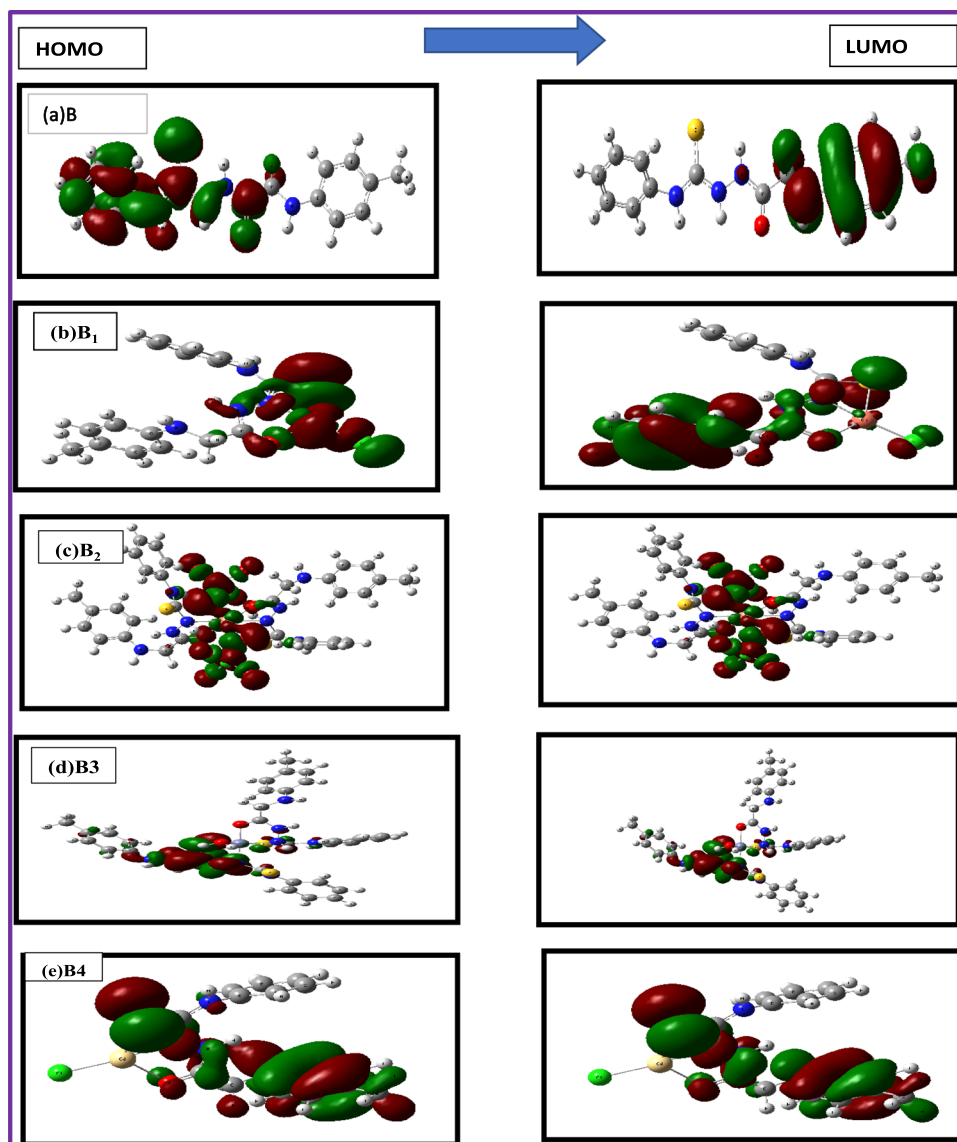


Table 6 Ground state properties of H₂L_B ligand using B3LYP/6-31G(+ +)d,p and its metal complexes using B3LYP/LANL2DZ

Parameter	H ₂ L	[Cu(H ₂ L)I]	[Cu(H ₂ L) ₂ (ClO ₄) ₂]	[Zn(H ₂ L) ₂ (H ₂ O)] SO ₄	[Cd(H ₂ L)Cl]Cl
E_T , Hartree	-1312.9304	-1135.3041	-2676.2810	-1991.3548	-986.9751
E_{HOMO} , eV	-5.22	-6.06	-6.04	-2.52	-9.06
E_{LUMO} , eV	-1.38	-3.88	-4.91	-1.72	-8.46
ΔE , eV	3.84	2.18	1.13	0.80	0.6
$I = -E_{HOMO}$, eV	5.22	6.06	6.04	2.52	9.06
$A = -E_{LUMO}$, eV	1.38	3.88	4.91	1.72	8.46
χ , eV	3.30	4.97	5.47	2.12	8.76
η , eV	1.92	1.09	0.565	0.4	0.30
S , eV ⁻¹	0.26	0.45	0.88	1.25	1.67
μ , eV	-3.30	-4.97	-5.47	-2.12	-8.76
Dipole moment (Debye)	3.2200	15.1634	3.2461	8.2389	15.7912

^a E : the total energy (a.u.), ^bHOMO: highest occupied molecular orbital (eV) and ^cLUMO: lowest unoccupied molecular orbital (eV), $\Delta E = E_{LUMO} - E_{HOMO}$

Fig. 8 Frontier HOMO and LUMO molecular orbitals for ligand **a** B = H₂L, **b** B₁ = [Cu(H₂L)]I, **c** B₂ = [Cu(H₂L)₂ClO₄], **d** B₃ = [Zn(H₂L)₂ClO₄] and **e** B₄ = [Cd(H₂L)Cl]Cl complexes calculated at DFT level



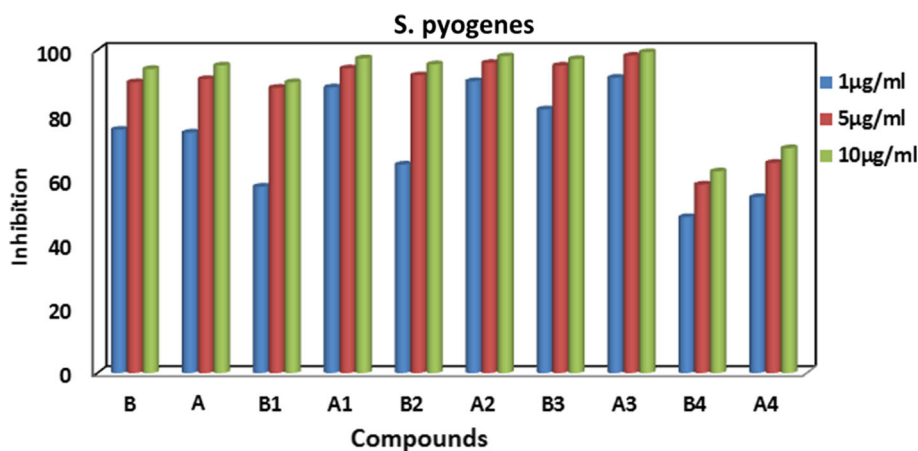
treatment of these diseases. In our study, we tested antibacterial activity of different copper, zinc and cadmium complexes as well as ligand (B, A) before and after irradiation on *E. coli* and *Streptococcus pyogenes* bacteria and data obtained showed a promising future in this branch of biotechnological application.

The synthesized ligand, Cu(I), Cu(II), Zn(II) and Cd(II) complexes (B and B₁–B₄) were separately exposed to gamma irradiation to test their improvement as active antibacterial drugs [47]. Results in Table S₁ and Figs. 9, 10 showed antibacterial activity against the tested microbes. Generally, it was found that antibacterial activity of both the synthetic ligand and metal complexes before and after γ -irradiation (B, B₁–B₄ and A, A₁–A₄) was proportionally increased with increased concentration. All compounds were tested starting from zero time of bacterial growth curve to examine the

effect of added concentrations throughout all the stages of growth. The tested compounds before and after γ -irradiation are found to have remarkable biological activity. In case of *E. coli*, that the corresponding Zn(II) and Cu(II) complexes showed much better antibacterial activity with respect to the individual ligand and complexes against the same microorganism under identical experimental conditions, the antibacterial activity of the tested compounds were found to follow the order: A₃ > A₂ > A₁ > B₃ > B₁ > B₂ > A > A₄ > B₄ > B for 1, 5 and 10 $\mu\text{g/ml}$ for before and after irradiation. On the other hand, antibacterial activity was recorded when using the ligand and metal complexes with *S. pyogenes* follow the order: A₃ > A₂ > B₃ > A₁ > B₂ > B₁ > A > B > A₄ > B₄ for before and after irradiation with 1 and 5 $\mu\text{g/ml}$ concentration [23, 48]. Obtained data showed more antimicrobial activity to *E. coli* than *S. pyogenes* corresponding to

Table 7 Some of the optimized bond lengths, Å and bond angles, degrees, for (H₂L) and its metal complexes using B3LYP/6-311G(+ +)d,p

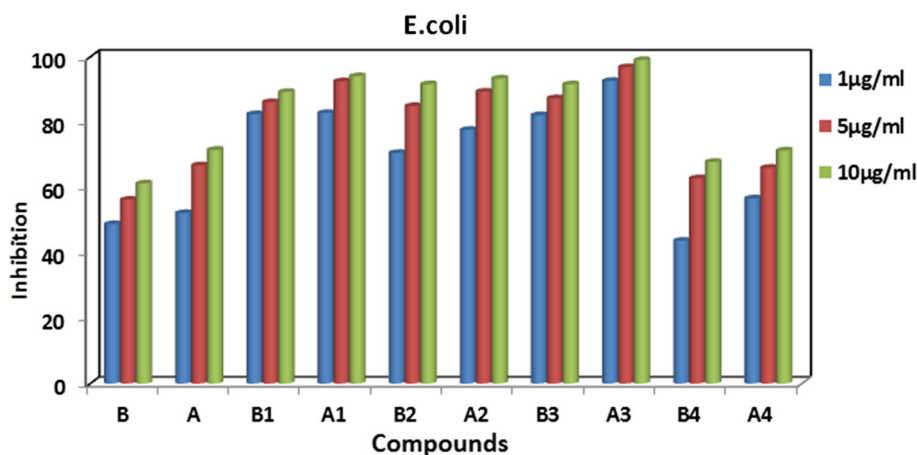
Bond length (A°)	H ₂ L	[Cu(H ₂ L)I]	[Cu(H ₂ L) ₂ (ClO ₄) ₂]	[Zn (H ₂ L) ₂ (H ₂ O)]SO ₄	[Cd(H ₂ LCl)Cl]
R (M–Cl)	–	2.19937	–	–	2.37881
R (M–O8)	–	2.22007	1.93603	2.06440	2.36369
R (M–N3)	–	1.96135	2.65910	2.04013	1.94974
R (M–OCIO ₃)	–	–	1.97195	–	3.04748
R (M–S1)	–	2.60876	–	2.37828	–
R (M–O–H ₂)	–	–	–	2.10239	–
R (C2–S1)	1.73273	1.80438	–	1.80719	1.46624
R (C5–O8)	1.25861	1.27510	1.27514	1.30843	1.45986
R (N4–C5)	1.35538	1.36229	1.34735	1.39788	1.32019
R (N3–C2)	1.36138	1.32646	1.46312	1.47620	1.35331
R (N7–C6)	1.44027	1.45935	1.45631	1.47188	1.45929
R (N9–C2)	1.37062	1.37303	1.34881	1.42723	1.36423
A (N3–M–Cl1)	–	175.483	–	–	68.909
A (Cl1–M–Cl2)	–	–	–	–	–
A (Cl1–M–O8)	–	108.139	–	–	118.508
A (O8–M–N3)	–	76.143	71.994	80.528	68.909
A (M–N3–N4)	–	118.525	98.360	103.377	118.280
A (M–O8–C2)	–	110.583	125.403	111.998	116.580
A (N3–M–O–ClO ₃)	–	–	98.448	–	–
A (O8–M–O–H ₂)	–	–	–	90.905	–
A (N3–M–S1)	–	66.774	–	81.522	–

Fig. 9 Antibacterial activity for ligand (B, A) and copper, zinc and cadmium (B₁, B₂, B₃, B₄ and A₁, A₂, A₃, A₄) complexes before and after irradiation against *S. pyogenes*

the hypothesis of the complexity of the cell wall structure of Gram-positive bacteria and Gram-negative bacteria [49]. The lipid membrane facilitates the passage of any fat-soluble substance, and liposolubility is known to be an important factor in controlling antibacterial activity. The results are consistent with the hypothesis that copper complexes may initially cause instability of the outer membrane, destroying the cell membrane, leading to bacterial cell lysis.

Results also suggested that in case of 1 µg/ml, 5 and 10 µg/ml Zn(II) and Cu(II) and complexes have higher activity than other complexes. The chelation could facilitate the ability to cross the cell membrane of *E. coli* and can be explained by Tweedy's chelation theory. Chelation/complexation could enhance the lipophilic nature of the central metal atom which in turn, favors its permeation through the lipid layer of the membrane thus causing the metal complex to cross the bacterial membrane more

Fig. 10 Antibacterial activity for ligand (B, A) and copper, zinc and cadmium (B₁, B₂, B₃, B₄ and A₁, A₂, A₃, A₄) complexes before and after irradiation *E. coli*



effectively thus increasing the activity of the complexes. Besides from this many other factors such as solubility, dipole moment, conductivity influenced by metal ion may be possible reasons for remarkable antibacterial activities of these complexes [50]. Exposure to gamma irradiation remarkably enhanced the antibacterial activity for both the ligand and its complexes when it was used in case of *E. coli*. Additionally, it also has been observed that some moieties such as N(2)H linkage introduced into such compounds exhibit extensive biological that may be responsible for increase in hydrophobic character and liposolubility of the molecules in crossing the cell membrane of the microorganism and enhance biological utilization ratio and activity of complexes activity [51]. The antibacterial studies of the prepared compounds screened against both Gram-positive and Gram-negative bacteria proved that these compounds exhibit remarkable antibacterial activity and can be used in the future as therapeutic drugs for pathogenic bacterial diseases.

3.9.1 The molecular docking

To understand the interaction of all the synthesized molecules with topoisomerase II DNA gyrase enzymes, the crystal structure of topoisomerase II was downloaded from Protein Data Bank (PDB ID: 2XCT) and the molecular docking studies were performed using the Moe program. The protein ligand interaction plays a significant role in structural based drug designing. The different types of interactions are mentioned in Table 8 and seen in Fig. 11. The preferred compounds Cd(II), Cu(II) and Zn(II) complexes had a scoring values of -5.02 , -9.41 and -10.87 , respectively. The Zn(II) complex showed the highest binding affinity and interaction with topoisomerase II DNA gyrase enzymes (2XCT) by using most types of protein binding interactions. The binding affinity of our compounds achieved higher or the same values numerous previous works against the same type of

Table 8 Comparison of binding affinity of metal complexes against topoisomerase II DNA gyrase enzymes (PDB Code: 2XCT)

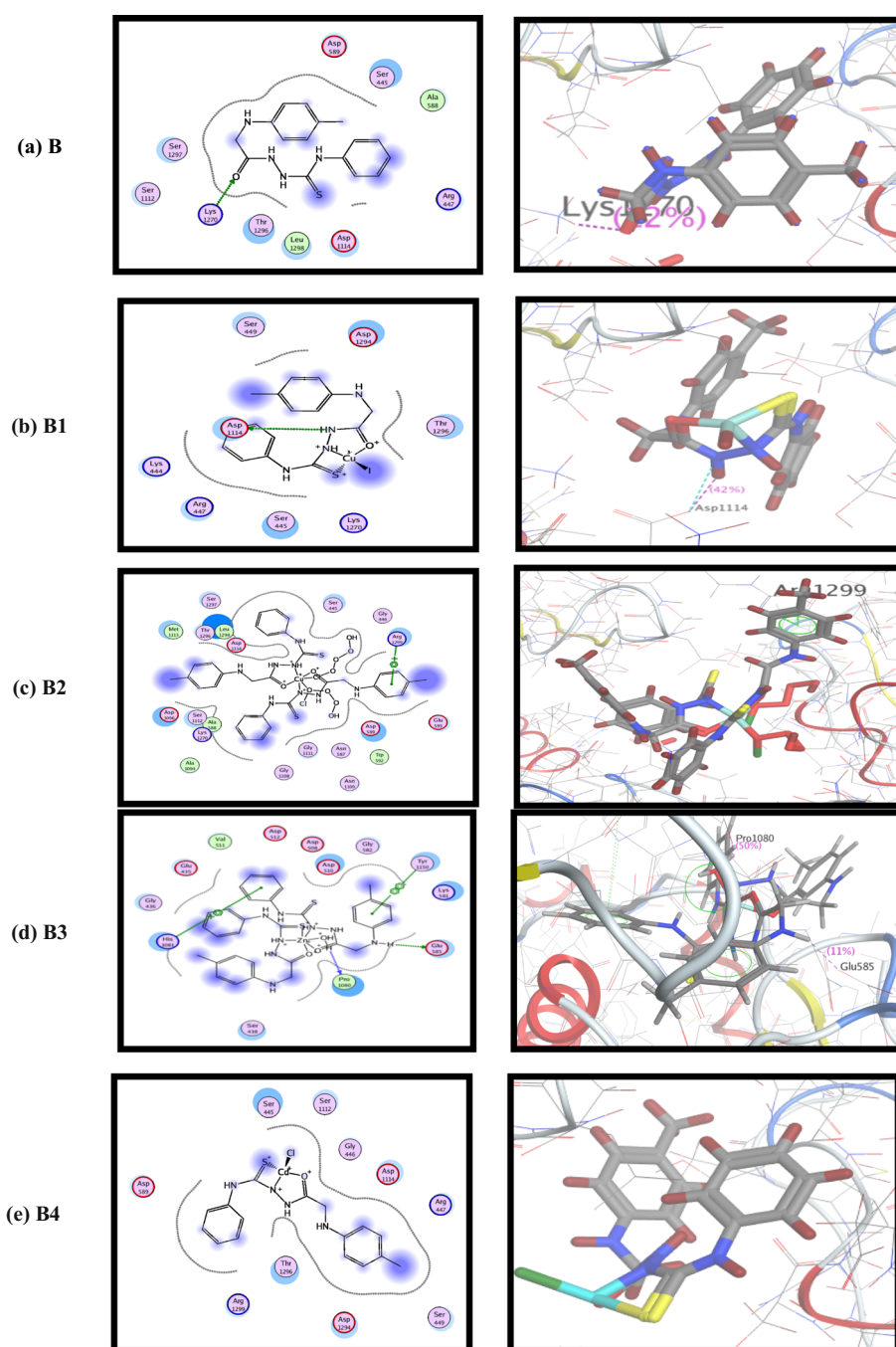
Compound	Involved amino acids (scoring energy)	Type of interaction
<i>Antitumor docking 4jsv</i>		
H ₂ L	Lys-1270 (-2.99)	Side chain donor
Cu(H ₂ L)I	Asp-1114 (-3.30)	Side chain acceptor
Cu(H ₂ L) ₂ (ClO ₄) ₂	Arg-1299 (-9.41)	Arene-cation interaction
[Zn (H ₂ L) ₂ (H ₂ O)]SO ₄	Glu-585, Pro-1080, Tyr-1150 and His-1081 (-10.87)	Side chain acceptor, Backbone acceptor, Arene-arene and Arene-cation
[Cd (H ₂ L)Cl]Cl	Ser1584 (-5.02)	Solvent contact

protein [52, 53]. The molecular docking of our work supported that the chelates are more active than their parent ligand against the same microorganism as mentioned also in many of our previous works [54].

4 Conclusions

New Cu(I), Cu(II), Zn(II) and Cd(II) complexes of *N*-phenyl-2-(*p*-tolylglycyl) hydrazine-1-carbothioamide (B) have been prepared and characterized by physical and analytical technique, and the effect of gamma irradiation on these compounds has been studied. The biological activities of unirradiated and irradiated compounds were investigated. And it turns out the following: the ligand behaves as neutral for tridentate, tetradentate coordinated to the ligand through the (C=O), N(2)H, (C=S) and coordination take place via two

Fig. 11 Binding pose of **a** B = H_2L , **b** B₁ = $[Cu(H_2L)I]$, **c** B₂ = $[Cu(H_2L)_2ClO_4]$, **d** B₃ = $[Zn(H_2L)_2ClO_4]$ and **e** B₄ = $[Cd(H_2L)Cl]Cl$ complexes in the active pocket of topoisomerase II DNA gyrase enzymes (PDB ID: 2XCT)



(C=O) and two N(2)H for complexes (B₂ and B₃), elemental analysis data indicated that the metal complexes have 1:1 (metal/ligand) (B₁ and B₄) or 1:2 stoichiometry for complexes (B₂ and B₃). X-ray diffraction patterns improve the crystallite size of the complexes by using gamma-irradiation. The proposed structures of complexes were geometrically optimized, also showed that the Cu(I), Cu(II), Zn(II) and Cd(II) complexes have four and six coordination geometries; this is also in a good agreement with the experimental

results. In vitro antibacterial activity of Zn(II) after irradiation complex has higher activity than other complexes, which indicates the extent to which gamma radiation affects the morphology and properties of matter.

Supplementary Information The online version contains supplementary material available at <https://doi.org/10.1007/s13369-023-07988-2>.

Author Contribution All authors equally contributed to the manuscript. They approved the final draft.

Data Availability The data that support the findings of this study are available in the supplementary material of this article.

Declarations

Conflict of Interest The authors declare no conflict of interest.

Open Access This article is licensed under a Creative Commons Attribution 4.0 International License, which permits use, sharing, adaptation, distribution and reproduction in any medium or format, as long as you give appropriate credit to the original author(s) and the source, provide a link to the Creative Commons licence, and indicate if changes were made. The images or other third party material in this article are included in the article's Creative Commons licence, unless indicated otherwise in a credit line to the material. If material is not included in the article's Creative Commons licence and your intended use is not permitted by statutory regulation or exceeds the permitted use, you will need to obtain permission directly from the copyright holder. To view a copy of this licence, visit <http://creativecommons.org/licenses/by/4.0/>.

References

- Khan, T., et al.: Anticancer potential of metal thiosemicarbazone complexes: a review. *Der Chem. Sin.* **6**(12), 1–11 (2015)
- Aly, S.A., et al.: Synthesis, spectroscopic characterization, thermal studies, and molecular docking of novel Cr(III), Fe(III), and Co(II) complexes based on Schiff base: in vitro antibacterial and antitumor activities. *J. Appl. Pharm. Sci.* **13**(2), 196–210 (2023)
- Tada, R.: Synthesis and characterization of some new thiosemicarbazide. *J. Chem. Pharm. Res.* **3**(2), 290–297 (2011)
- Al-Karawi, A.J.M.; Al-Dulimi, A.A.A.; Al-Mokaram, A.M.A.A.: Synthesis, characterization and thermal properties of sodium pyruvate thiosemicarbazone and some of its metal complexes. *J. King Saud Univ. Sci.* **24**(1), 25–31 (2012)
- Abdalla, E.M., et al.: Molecular docking, DFT calculations, effect of high energetic ionizing radiation, and biological evaluation of some novel metal (II) heteroleptic complexes bearing the thiosemicarbazone ligand. *Molecules* **26**(19), 5851 (2021)
- Abou Sekkina, M.M.; Kashar, T.I.; Aly, S.A.: Spectrochemical study and effect of high energetic gamma ray on copper(II) complexes. *Solid State Sci.* **13**(12), 2080–2085 (2011)
- Abou Sekkina, M.; El-Boraey, H.; Aly, S.: Further studies on the properties and effect of high energetic ionizing radiation on copper(II) complexes: 1H NMR, electronic absorption, ESR spectra and solid electrical conductivity. *J. Radioanal. Nucl. Chem.* **300**(2), 867–872 (2014)
- Aly, S.; Elembaby, D.: Synthesis, spectroscopic characterization and Study the effect of gamma irradiation on VO²⁺, Mn²⁺, Zn²⁺, Ru³⁺, Pd²⁺, Ag⁺ and Hg²⁺ complexes and antibacterial activities. *Arab. J. Chem.* **13**(2), 4425–4447 (2020)
- El-Boraey, H.A.; Abdel-Hakeem, M.A.: Facile synthesis, spectral, EPR, XRD and antimicrobial screening of some γ -irradiated N', N''-(1E, 2E)-1, 2-diphenylethane-1, 2-diylidene) bis (2-aminobenzohydrazide) metal complexes. *J. Mol. Struct.* **1211**, 128086 (2020)
- El-Boraey, H.; El-Gammal, O.; Abdel Sattar, N.: Impact of gamma-ray irradiation on some aryl-amide-bridged Schiff-base complexes: spectral, TGA, XRD, and antioxidant properties. *J. Radioanal. Nucl. Chem.* **323**(1), 241–252 (2020)
- Alshater, H., et al.: Improving the surface morphology and crystallite size of isonicotinohydrazide based binuclear Cr(III), Zn(II) and Sn(IV) complexes after irradiation with γ -rays. *J. Mol. Struct.* **1232**, 129985 (2021)
- West, T.S.; West, T.: *Complexometry with EDTA and related reagents*. Vol. 46. BDH Chemicals Limited. (1969)
- Frisch, M., et al.: *Gaussian 09, rev. A. 02*. Gaussian, Inc., Wallingford (2009)
- Aly, S.; El-Boraey, H.A.: Effect of gamma irradiation on spectral, XRD, SEM, DNA binding, molecular modeling and antibacterial property of some (Z) N-(furan-2-yl) methylene)-2-(phenylamino) acetohydrazide metal (II) complexes. *J. Mol. Struct.* **1185**, 323–332 (2019)
- Elhalafawy, K., et al.: Purification and characterization of streptokinase produced by *S. pyogenes* and *S. equisimilis*. *Sci. J. Fac. Sci. Minu Univ.* **23**, 85–103 (2009)
- Chemical Computing Group, M.: *Molecular operating environment*. Chemical Computing Group Montreal, Quebec, (2008)
- Alshater, H., et al.: Antitumor and antibacterial activity of Ni(II), Cu(II), Ag(I), and Hg(II) complexes with ligand derived from thiosemicarbazones: characterization and theoretical studies. *Molecules* **28**(6), 2590 (2023)
- Abdalla, E.M., et al.: Synthesis, characterization, theoretical studies, and antimicrobial/antitumor potencies of salen and salen/imidazole complexes of Co(II), Ni(II), Cu(II), Cd(II), Al(III) and La(III). *Appl. Organomet. Chem.* **34**(11), e5912 (2020)
- Kong, D.; Xie, Y.: Synthesis, structural characterization of tetraaza-macrocyclic ligand, five-coordinated zinc(II) complex. *Inorg. Chim. Acta.* **338**, 142–148 (2002)
- Geary, W.J.: The use of conductivity measurements in organic solvents for the characterisation of coordination compounds. *Coord. Chem. Rev.* **7**(1), 81–122 (1971)
- Aly, S.A.: Spectrochemical study the effect of high energetic ionization radiation on Ru(III), Pd(II) and Hg(II) complexes. *J. Radiat. Res. Appl. Sci.* **10**(2), 89–96 (2017)
- Vikneswaran, R., et al.: New alicyclic thiosemicarbazone chelated zinc(II) antitumor complexes: interactions with DNA/protein, nuclease activity and inhibition of topoisomerase-I. *Polyhedron* **105**, 89–95 (2016)
- El-Boraey, H.A.; El-Salamony, M.A.; Hathout, A.A.: Macrocyclic [N5] transition metal complexes: synthesis, characterization and biological activities. *J. Incl. Phenom. Macrocycl. Chem.* **86**(1), 153–166 (2016)
- Aly, S.A., et al.: Quantum chemical studies and effect of gamma irradiation on the spectral, thermal, X-ray diffraction and DNA interaction with Pd(II), Cu(I), and Cd(II) of hydrazone derivatives. *Appl. Organomet. Chem.* **35**(4), e6153 (2021)
- Seenaa, E.; Kurup, M.P.: Synthesis, spectral and structural studies of zinc (II) complexes of salicylaldehyde N (4)-phenylthiosemicarbazone. *Spectrochim. Acta A Mol. Biomol. Spectrosc.* **69**(3), 726–732 (2008)
- Ra, U., et al.: Metal complexes of tetradentate azo-dye ligand derived from 4, 4'-oxydianiline: preparation, structural investigation, biological evaluation and MOE studies. *Appl. Organomet. Chem.* **33**(7), e4946-4966 (2019)
- Pathaw, L., et al.: Tetrahedral copper (I) complexes of novel N, N-bidentate ligands and photophysical properties. *Inorg. Chim. Acta.* **514**, 119999 (2021)
- Majeed, A.; Alabdeen, K.: Synthesis and characterization of new thio-triazole ligand and complexes with selected metals. *J. Phar. Bio. Sci. (IOSR-JPBS)* **4**(5), 09–14 (2012)
- Sharma, M., et al.: Octahedral copper(ii)-diimine complexes of triethylenetetramine: effect of stereochemical fluxionality and ligand hydrophobicity on Cu II/Cu I redox, DNA binding and cleavage, cytotoxicity and apoptosis-inducing ability. *Dalton Trans.* **49**(24), 8282–8297 (2020)
- LeBlanc, M.-A., et al.: Coordination chemistry of polyaromatic thiosemicarbazones 2: synthesis and biological activity of zinc,

- cobalt, and copper complexes of 1-(naphthalene-2-yl) ethanone thiosemicarbazone. *Int. J. Inorg. Chem.* **624756**, 1–8 (2011)
31. Paira, M., et al.: Zn(II), Cd(II) and Hg(II) complexes of 8-aminoquinoline. Structure, spectra and photoluminescence property. *Polyhedron* **26**(15), 4131–4140 (2007)
 32. Azam, M.; Al-Resayes, S.I.; Pallepogu, R.: Synthesis and structural characterization of Cadmium(II) and Mercury(II) complexes derived from 3-aminoquinoline. *Helv. Chim. Acta* **99**(1), 20–23 (2016)
 33. Sen, S., et al.: Synthesis and structure of a heptacoordinated cadmium (II) complex. *Inorg. Chim. Acta.* **288**(1), 118–121 (1999)
 34. Abdel-Rahman, L.H., et al.: Synthesis, characterization, potential antimicrobial, antioxidant, anticancer, DNA binding, and molecular docking activities and DFT on novel Co(II), Ni(II), VO(II), Cr(III), and La(III) Schiff base complexes. *Appl. Organomet. Chem.* **36**(1), e6484 (2022)
 35. Al-Farhan, B.S., et al.: Synthesis, DFT calculations, antiproliferative, bactericidal activity and molecular docking of novel mixed-ligand salen/8-hydroxyquinoline metal complexes. *Molecules* **26**(16), 4725 (2021)
 36. Huang, B.-L., et al.: Formation of supersaturated solid solutions by mechanical alloying. *Nanostruct. Mater.* **7**(1–2), 67–79 (1996)
 37. Al-Ashqer, S., et al.: Spectral studies on a series of metal ion complexes derived from pyrimidine nucleus, TEM, biological and γ -irradiation effect. *Spectrochim. Acta A Mol. Biomol. Spectrosc.* **132**, 751–761 (2014)
 38. Jayashri, T.; Krishnan, G.; Rema Rani, N.: Effect of gamma-irradiation on thermal decomposition kinetics, X-ray diffraction pattern and spectral properties of tris (1, 2-diaminoethane) nickel (II) sulphate. *Radiat. Eff. Defects Solids* **169**(12), 1019–1030 (2014)
 39. Jeslin Kanaga Inba, P., et al.: Cu(II), Ni(II), and Zn(II) complexes of salan-type ligand containing ester groups: synthesis, characterization, electrochemical properties, and in vitro biological activities. *Bioinorg. Chem. Appl.*, (2013)
 40. Sharma, A.; Shah, M.: Synthesis and characterization of some transition metal complexes derived from bidentate Schiff base ligand. *J. Appl. Chem.* **3**(5), 62–66 (2013)
 41. Hassan, S.S.: Antibacterial, DFT and molecular docking studies of Rh (III) complexes of Coumarinyl-Thiosemicarbazone nuclei based ligands. *Appl. Organomet. Chem.* **32**(3), e4170 (2018)
 42. Hassan, S.S.; Gomha, S.M.: Novel functionalized thiosemicarbazone ligands and their Pd(II) complexes: synthesis, characterization, antibacterial and cytotoxic activities. *Chem. Pap.* **73**(2), 331–344 (2019)
 43. Hassan, S.S.; Mohamed, E.F.: Antimicrobial, antioxidant and anti-tumor activities of nano-structure Eu(III) and La(III) complexes with nitrogen donor tridentate ligands. *Appl. Organomet. Chem.* **34**(2), e5258 (2020)
 44. Warnes, S., et al.: Biocidal efficacy of copper alloys against pathogenic enterococci involves degradation of genomic and plasmid DNAs. *Appl. Environ. Microbiol.* **76**(16), 5390–5401 (2010)
 45. Zhu, L., et al.: Antimicrobial activity of different copper alloy surfaces against copper resistant and sensitive *Salmonella enterica*. *Food Microbiol.* **30**(1), 303–310 (2012)
 46. Yazdankhah, S.; Rudi, K.; Bernhoft, A.: Zinc and copper in animal feed—development of resistance and co-resistance to antimicrobial agents in bacteria of animal origin. *Microb. Ecol. Health Dis.* **25**(1), 25862 (2014)
 47. Tweedy, B.: Plant extracts with metal ions as potential antimicrobial agents. *Phytopathology* **55**, 910–914 (1964)
 48. Sönmez, M.; Celebi, M.; Berber, I.: Synthesis, spectroscopic and biological studies on the new symmetric Schiff base derived from 2, 6-diformyl-4-methylphenol with N-aminopyrimidine. *Eur. J. Med. Chem.* **45**(5), 1935–1940 (2010)
 49. Qi, J., et al.: Synthesis, antiproliferative activity and mechanism of copper (II)-thiosemicarbazone complexes as potential anticancer and antimicrobial agents. *J. Coord. Chem.* **73**(7), 1208–1221 (2020)
 50. Chohan, Z.H., et al.: Antibacterial, antifungal and cytotoxic properties of novel N-substituted sulfonamides from 4-hydroxycoumarin. *J. Enzyme Inhib. Med. Chem.* **21**(6), 741–748 (2006)
 51. Singh, A., et al.: Manganese(II) and zinc(II) complexes of 4-phenyl (2-methoxybenzoyl)-3-thiosemicarbazide: synthesis, spectral, structural characterization, thermal behavior and DFT study. *Polyhedron* **73**, 98–109 (2014)
 52. Pisano, M.B., et al.: Antibacterial activity and molecular docking studies of a selected series of hydroxy-3-aryl coumarins. *Molecules* **24**(15), 2815 (2019)
 53. El-Etrawy, A.-A.S.; Sherbiny, F.F.: Design, synthesis, biological assessment and molecular docking studies of some new 2-Thioxo-2, 3-dihydropyrimidin-4 (1H)-ones as potential anticancer and antibacterial agents. *J. Mol. Struct.* **1225**, 129014 (2021)
 54. Khalf-Alla, P.A., et al.: Synthesis, characterization, speciation, and biological studies on metal chelates of carbohydrates with molecular docking investigation. *Macromol. Mater. Eng.* **306**(3), 2000633 (2021)

